MASTER THESIS

MEASURING THE ASSISTANCE PROVIDED BY SENSORIZED PASSIVE BACK-ASSIST EXOSUITS DURING INDUSTRIAL APPLICATIONS

Swathika Subramanian

FACULTY OF ENGINEERING TECHNOLOGY
DEPARTMENT OF BIOMECHANICAL ENGINEERING

EXAMINATION COMMITTEE
PROF.DR.IR. M. SARTORI
DR.IR. M.I. REFAI
S.S. SHEIKH ABOUMASOUDI

DOCUMENT NUMBER
-

UNIVERSITY OF TWENTE.

OCTOBER
2024

Measuring the assistance provided by sensorized passive back-assist exosuits during industrial applications

Abstract—**Low-back pain is a commonly reported health problem amongst industry workers due to peak mechanical loading of the spine. Forces exerted by back-assist exosuits can mitigate peak compression loading and muscle workload. To ensure optimal force transmission to the user, measuring human-exosuit interaction forces is necessary. Existing methods include indirect representation of exosuit forces that involved multiple assumptions and deployment of computationally expensive tools. Alternatively, direct methods utilizing physical sensors can provide instantaneous measurements with minimal setup requirements. Hence, this study aimed at measuring passive exosuit forces exerted on the user's trunk from two industrial exosuits using a sensor-based approach. Furthermore, the measured interaction forces were related to marker-based forces, user's back muscle activity and anthropometry. The two industry exosuits used were Darwing and Auxivo.Ten participants performed tasks primarily involving stoop and squat movements that are often associated with industry tasks. Data from force sensors/load cells, EMG sensors and optical markers were collected. Results showed significant difference in interaction forces only for stoop trials in both exosuits. Comparing load cell and marker forces showed significant difference in dynamic trials with Auxivo. Effect of trunk flexion angles and interaction forces on muscle activations were minimal. Inter-subject variability in interaction forces were due to difference in shoulder-width across users. Thus, measuring interaction forces provided insightful information about performance of the exosuits and its effect on physiological parameters.**

Index Terms—**Soft passive exosuits, load cells, optical markers, EMG**

I. Introduction

Despite advancements in technology and automation in industries, manual handling of loads is still a common practice leading to several back-related musculoskeletal disorders [1], [2]. More than 40% of the working population in EU suffer from low-back pain (LBP) [1].
Peak compression loading of the spine is a common cause of LBP as reported by industry safety and regulation guidelines [3]. For preventing the onset of LBP in industrial workers, measures such as promoting the use of cranes and jibs and periodic assessments on body postures and load lifting techniques were undertaken in occupational settings [4], [5]. Nonetheless, some of these were disregarded due to high cost of installation and infeasibility.

A recent intervention involving wearable assistive devices was considered a practical alternative to support industry workers in their regular tasks [6]. Back-assist wearable devices, also known as back-assist exoskeletons, play a crucial role in mitigating intense activity of back muscles that are often the cause of peak spinal compression loading [7]. In terms of actuation techniques to support back muscles, both powered/active and passive exoskeletons have been extensively developed for occupational use [4]. Passive exoskeletons use elastic elements like springs or bands for actuation that store energy from user's movement and release when required [4]. Soft passive exosuits are a subset of this group, that fit to user's body like a garment and offer support without hindering natural movements, thereby, increasing user comfort [4], [8]. These exosuits supporting the trunk, generate assistive forces from the deformation of elastic elements, in a direction approximately parallel to the direction of back muscle forces leading to reduction in peak muscle activity and compression loading [6] - [8]. However, such passive assistive forces should be monitored to prevent detrimental effects to the user. For instance, higher assistive forces may offer greater assistance but at the expense of damage to underlying biological tissues, user comfort and experience with the device [6], [9]. On the other hand, lower assistive forces may not adequately support the lower back muscles and minimize the peak compression loads [10]. Hence, to evaluate the functionality of soft passive exosuits, computation of assistive or interaction forces provided by the exosuit is necessary. Quantitative data on such assistive forces can also benefit exosuit designers and manufactures to refine some design aspects such as spring stiffness or slack length to maximize assistance to the user while ensuring safety [9].

Studies have revealed different methods to measure the human-exosuit interaction forces. These include indirect measurements utilizing motion capture (MoCap) system, modelling techniques such as simulation and mathematical models, and direct measurements incorporating physical sensors. One study used the marker-based approach to measure the exosuit assistive forces [5]. Reflective markers were placed on the anchoring points of the elastic bands to the exosuits to measure the elongation of the band at different stretch levels. A force-elongation relationship was then established to extract the stretch forces generated by the elastic band. However, the elongation measured was linear and therefore, did not account for the force distribution when the elastic band bent along with the curvature of trunk during forward bending. Additionally, forces were estimated from polynomial interpolation curves that may not represent the actual forces acting on the user. Another study driven by kinematic data from MoCap system developed a spring model at the interface of lower limb and simulated passive exoskeleton [11]. However, the passive actuation mechanism of the modelled spring resulted in generation of perpendicular forces as observed in passive rigid exoskeleton and not passive soft exosuit that produces forces tangentially across the body segment it spans. Moreover, marker-based system require extensive laboratory setup [12].

Mathematical models to explain the interaction forces in terms of mechanical model parameters such as displacements, center of rotations have been studied [13]. However, such analytical methods were simplified representations and did not account for the complex dynamics presented by the elastic elements of the wearable suits or the viscoelastic properties of the soft tissues.

Simulation-based methods for modelling human-exoskeleton interaction forces included a virtual representation of the wearable device coupled with the human musculoskeletal model [14]. Such an approach was developed to present the realistic behaviour of the wearable device on the user without human involvement in testing and early prototype designing. The interaction forces were simulated using spring-damper system similar to [11] with constant stiffness and damper coefficients. However, these modelled forces were observed even when the system was set apart from the human model. Hence, this method was not representative of actual device behaviour. Another method that tackled this issue by measuring forces only at contact points, was defined as a modelling-heavy task [14]. Moreover, these modelling methods had extensively analysed powered/passive exoskeletons thus, focussing on normal forces as opposed to tensile forces exerted by elastic elements of exosuits. Hence, extrapolating conceptual ideas from these models to compute soft exosuit forces may not be suitable as their design configurations and modelling techniques are not comparable with those of exosuits. Furthermore, these models utilized computationally expensive tools that are often time consuming.

Sensor-based system is a simple and an effective tool for instantaneous measurements of quantities and are often exploited in the field of rigid exoskeletons [15]. Exosuits can apply pressure over the contact area on the user's body. Pressure sensors and force sensitive resistors (FSRs) can be used for sensing forces generated due to contact pressure [14] - [16]. But back-assist exosuits in general, have passive elements that cover the entire length of the user's trunk. Hence, multiple pressure sensors and FSRs would be required to compute the resultant tensile force acting on the trunk, making the setup complicated and expensive. To avoid this, soft tactile sensor and customized force sensors [17], [18] have been proposed to quantify forces from pressure distribution across the user-device interface. However, such sensors require meticulous fabrication process and are also susceptible to normal forces. Conventional uniaxial force sensors have been used in some studies for measuring tensile forces from elastic elements of the exosuit [4], [19], [20] and have resulted in precise measurements. However, these studies developed prototypes and to the best our knowledge, did not implement the setup in existing industrial exosuits. Hence, the primary research goal of the study is: Can we design a sensor-based system for objectively measuring human-exosuit forces in industrial exosuits? The secondary outcome includes: How different are these interaction forces when compared to marker-based estimation? The effects of interaction forces on physiological parameters include: Can we relate the measured interaction forces to muscle activity? Do the measured forces differ with variations in anthropometric measurements between individuals?

The study will incorporate sensor-based methodology using conventional force sensors with two industrial soft passive exosuits namely, Darwing Hakobelude (Daiya Industry Co., Ltd., Okayama, Japan) and Auxivo Liftsuit 1.0 (Auxivo, Schwerzenbach, Switzerland).

We hypothesize that: 1) Interaction forces from sensors vary from that of marker-based estimation 2) Muscle activations are influenced by interaction forces 3) Interaction forces are affected by difference in anthropometry.

TABLE I: Specifications of the soft exosuits used in the study. The table adapted from [5]

	Darwing Hakobelude	**Auxivo Liftsuit 1.0**
Short Name	Darwing	Auxivo
Company	Daiya Industry Co.	Auxivo AG
Weight (kg)	0.8	0.9

II. METHODS

A. *Exosuit specifications*

Table 1 and Figure 1 describes the two soft exosuits specifications. The Darwing exosuit has two textile elastic bands on each side that covers the upper interface to support the trunk and two on each side that covers the lower interface to support the lower limbs. Auxivo exosuit has two textile elastic bands on the upper back that connect to the thigh cuffs through adjustable straps to collectively support the upper back and thighs.

B. *Prototype Design*

Figure 1 shows the two soft passive exosuits with load cells attached. Miniature load cells were used for its compact size (S610 Miniature Load Cell, Strain Measurement Devices, Wallingford, CT, USA). These load cells were placed in series with each of the elastic bands to measure the stretch force directly upon elastic deformation. In Darwing, shown in Figure 1a, the load cells were placed only on the two elastic bands of the upper interface as the elastic bands of the lower interface could not be detached from the suit. One end of the load cell was drilled to the elastic band that is mobile and the other end of the cell

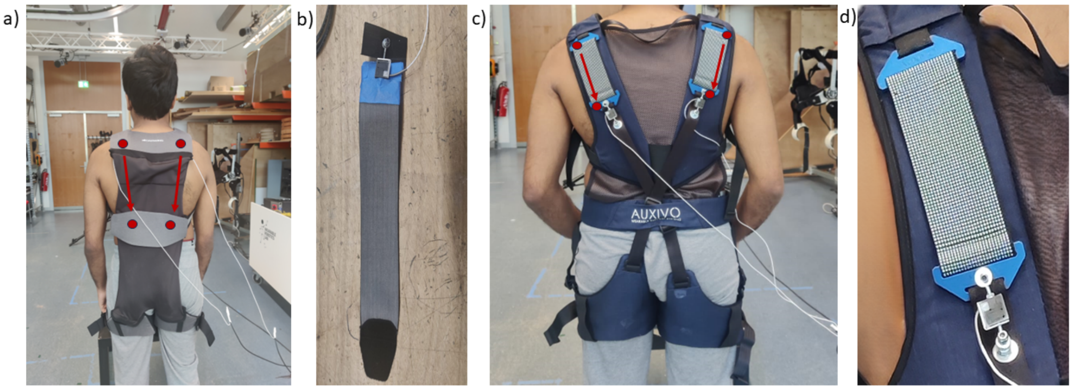

Fig. 1: a) Darwing exosuit with load cells attached to the elastic bands situated inside the exosuit. b) Load cell attached to one end of an isolated elastic band from the Darwing exosuit. c) Auxivo exosuit with 2 load cells attached to elastic bands. d) A close-up snapshot of the load cell attached to elastic band in Auxivo. The red arrows on both exosuits indicate the line of action of stretch force and the red dots are optical markers on the anchoring points of the exosuits.

was drilled to a stationary velcro extension as shown in the Figure 1b. Stretching of elastic band creates a tension in the load cell that leads to the part of the load cell connected to the elastic band (mobile part) to expand and the other part connected to the velcro extension to contract (stationary part). The resistive force generated due to tension is measured through load cells. In Auxivo, the load cells were drilled to the metal part of the elastic band on one end and to straps on the other as shown in Figure 1c. The force upon stretching of the elastic band was measured through load cells.

C. *Load cell circuit setup*

Load cells are simple and reliable for measuring tensile and compression loads. These are manufactured in various sizes to be widely used in different settings. Load cell acts as a transducer that converts physical quantities such as force and weight into a measurable electrical signal such as voltage [21]. Load cell is composed of strain gauges that are connected to each other in a bridge configuration. The bridge functions with a 5 volts(V) external DC power supply. When the load cell is subjected to external load or tension, the bridge undergoes instability and outputs a small voltage in response. Normally, the output voltage generated from the load cell is in the range of millivolts (mV). Hence, each load cell was coupled with an instrumentation amplifier. This study used a 24-bit ADC HX711 amplifier (Sparkfun, Niwot, CO, USA). This amplified the analog voltage inputs with a gain of 128 and converted those to corresponding digital values (signal conditioning). The default sampling rate of the amplifier was 10Hz which was up-sampled to 80Hz by altering an internal amplifier board connection. The manufacturer of HX711 amplifier had published an open-source script online [22] to interface the amplifier with Arduino Mega 2560 microcontroller (Arduino AG, Turin, Italy). The digital output from the amplifier was connected to the input digital ports of the Arduino. The Arduino was externally powered through laptop via USB cable. Libraries to recognize HX711 output ports were installed in the Arduino software and the open-source script was implemented. The script contained input parameters such as calibration factor and offset/zero factor that computed forces from the digital values. In general, force is calculated by the equation:

$$\text{Force (N)} = \frac{\text{Raw digital value} - \text{offset}}{\text{calibration factor}}$$

Raw digital value(bits) is the reading obtained at every instance, offset(bits) is the initial baseline value that is read when the load cell is under zero stress and calibration factor(bits/N) is a constant value that is obtained through a separate load cell calibration experiment. The script contained inbuilt functions to carry out the above calculation and returned forces in Newtons as output.To copy and save the output values, an open-source terminal emulator called PuTTY was used. The output force values from Arduino were transferred through serial communication (COM port) to PuTTY terminal and the force values were stored in usual file formats.

1) Load cell calibration experiment: Before recording data from load cells, calibration of load cells is necessary for reliable measurements [23]. This is a one-time procedure to set the calibration factor unless the positions of load cells are altered. Known weights in kg or N were suspended from the elastic band creating a stretch. The calibration factor responsible for force calculation was scaled or adjusted until the reading matched the known force value. This was done for all load cells in both exosuits and were incorporated in the script accordingly.

The designed prototypes with calibrated load cells were evaluated through experiment trials with human subjects.

D. *Experiment protocol*

1) Participant information:

9 participants (height in cm: 173.8 ± 11.1, weight in kg: 73.4 ± 16.5, age in years : 23.5 ± 1.4) with no previous experience with exosuits and with no history of back injuries participated in the study. Besides the 9, one participant (height: 186cm, weight: 84kg, age: 70 years) belonging to a different age group also took part in the data collection (refer to Appendix C). All participants provided informed consent. The Natural Sciences and Engineering Sciences Ethics committee of the University of Twente approved this experiment protocol (ref.number: 240424)

2) Apparatus:

For this study, data from the load cells, reflective markers (Qualisys Medical AB, Gothenburg, Sweden), ground reaction forces (1 AMTI force plate, MA, USA), wireless inertial measurement units (IMUs) (Xsens Technologies B.V., Enschede, Netherlands) and wireless surface EMG sensors from COMETA (Picolite EMG, Milan, Italy) were collected. 5 EMG sensors were placed on 3 bilateral dorsal muscles: Longissimus Thoracis pars Thoracis (LT-R,LT-L), Longissimus Thoracis pars Lumborum (LL-R,LL-L), and right Iliocostalis Lumborum (IL-R). 63 optical markers were placed on the participant. 56 full-body markers on bony landmarks and body segments and 7 on the each exosuit. 17 full-body IMU sensors were placed on the subject. Data from IMUs were visualized using the analyze software for trunk and knee joint angles during static hold trials. Marker data were sampled at 128 Hz, EMG data at 2048 Hz and load cell data at 80Hz. Manual synchronization of Arduino and Qualysis system was implemented to compare load cell, marker and EMG data at same time sequences.

3) Experiment procedure:

After placement of EMG sensors, IMUs and markers, subjects were asked to perform maximum voluntary contraction (MVC) trial to maximally activate the back muscles and IMU calibration. After this, the shoulder and thigh straps of the exosuits were adjusted to ensure maximum tight fit to the user. The tasks were performed with both Darwing and Auxivo exosuit. The tasks primarily involved two movements in the sagittal plane namely, stoop and squat that are often associated with industry tasks [24].

1) *Static hold trials:* Participants were asked to perform stoop at predefined trunk flexion angles of 40°, 60° and 80°, hold for 3 seconds and return to back erect posture. These *static stoop* trials were named as *stoop40*, *stoop60*, *stoop80* respectively. Similarly, participants were asked to perform squat at predefined knee flexion angles of 70°, 90° and 110°, hold for 3 seconds and return to back erect posture. These *static squat* trials were named as *squat70*, *squat90*, *squat110* respectively. The *static squat* and *stoop* movements were repeated thrice each.

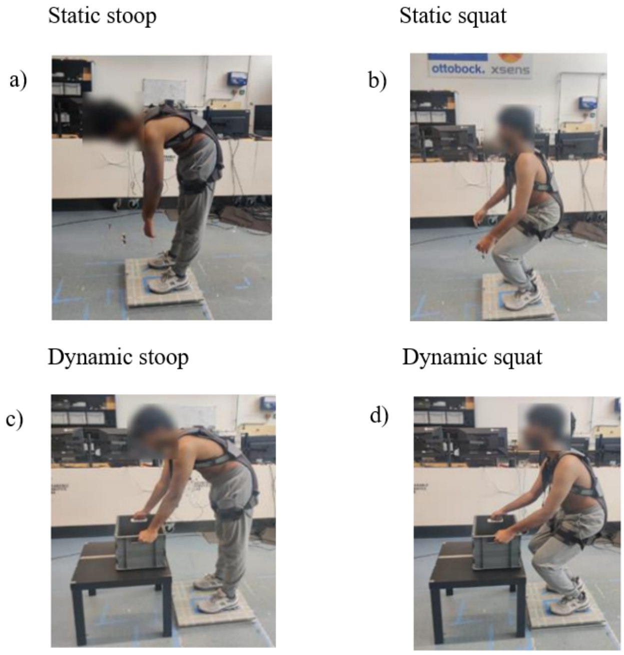

Fig. 2: a) Subject performing forward bend with minimal knee flexion b) Subject performing squat with minimal trunk flexion. c) Subject performing stoop lifting technique with a box d) Subject performing squat lifting technique with a box

2) *Dynamic trials:* Participants were asked to perform stoop where they flexed their trunk to lift an empty box from a table placed in front of the them, returned to back erect posture and again flexed their trunk to place the box back on the table. Similarly, participants did squat by flexing their knee to lift an empty box from a table placed in front of the them, returned to back erect posture and again flexed their knee to place the box back on the table. The two trials were named as *dynamic stoop* and *dynamic squat* respectively. Additionally, *dynamic squat* with 5kg weight and *dynamic squat* with roughly 50% assistance from the exosuit (loosening the straps to 50% disengagement of the suit) were performed. The *dynamic squat* and *stoop* lifting movements involved 5 repetitions each at 40 beats/min using metronome.

E. Data Analysis

Data from 9 participants were analysed. Participant from the industry was dealt separately in a case-study due to difference in age and occupation when compared to others.

Data from the single force plate were inconsistent with varying magnitude during the trials and were removed from analysis.

Data from a total of 20 trials including both exosuits per subject were collected. To reduce complexity of analysis, data from only selected trials were used for analysing parameters under each section.

1) Load cell data: The data was filtered by a zero-lag second order butterworth low pass filter of 6Hz. Forces from load cells on both sides of the exosuits were averaged across all participants. To obtain the resultant force acting on the trunk of the user, the measured interaction forces of the right and left elastic bands were summed. Previous study [5] had determined 118 N to be the force that resulted in maximum elongation of each elastic band in both exosuits which means, 236 N (multiplying 118 twice for two elastic bands) could be the maximum force that can be provided to the user's trunk by each exosuit. Thus, the summed up load cell forces from each exosuit were normalized to 236 N and were represented in percentages. The peak of these normalized forces were used for further analysis.

2) Marker data: Raw marker data were filtered by a zero-lag second order butterworth low pass filter of 6Hz. In this study, marker data was used for computing stretch forces of elastic bands and joint angles of trunk and knee. Previous approach described in [5] for the estimation of forces using markers on the exosuits as shown in Figure 1 were implemented to compare with forces obtained from load cells. The distance between the markers placed on either end of each elastic band was considered as band elongation and was fed to two polynomial equations representing the loading (flexion) and unloading (extension) phase of a task cycle to estimate forces for each exosuit. The loading and unloading phase of a cycle was determined using gradient (slope) of the curve. Positive and negative slope marked the start of loading and unloading phases of a task cycle respectively. The constant in the polynomial equation resulted in forces to be shifted by that value from zero. Hence, the constant in the loading equation was subtracted from the calculated forces. The estimated forces from the two elastic bands were summed and averaged across all participants for both exosuits.

The trunk and knee joint angles were computed using marker trajectories in the 2-D sagittal plane. For trunk inclination, angle between the vector joining the markers C7 and right posterior superior iliac and an arbitrary vector perpendicular to ground was measured. The initial alignment of one vector relative to another did not result in 180°, giving rise to an offset. To remove this, the measured angle was subtracted from the angle between these two vectors in neutral pose trial (generally used for scaling in Opensim). Similarly, knee flexion angles were computed using two vectors joining right anterior superior iliac-right lateral femoral epicondyl and right lateral femoral epicondyl-right lateral malleolus. The initial angle between the two vectors was not 0°. Hence, the angle between the vectors in neutral pose was subtracted from the measured knee flexion angles.
Furthermore, to find the relationship between interaction forces and anthropometry, various trunk measurements were obtained from the markers placed on the users. Measurements related to the user's trunk could explain the inter-subject variability in interaction forces if present.

3) EMG data: Raw EMG data from each channel was filtered using a zero-lag second order band pass butterworth filter with cut-off frequencies of 30 and 300Hz. This was followed by full wave rectification to obtain absolute values of the signal. Linear envelope was then extracted by passing a second order low pass butterworth filter of 6Hz. The processed EMG signals were normalized to MVC of the muscles. EMG signals from the muscles were averaged across all participants. Root mean square (RMS) of the whole lifting cycle of *dynamic stoop* and *squat* trials were measured. Peak EMG values were extracted between the interval 40-70% of a task cycle. Trunk muscle activations are also influenced by trunk and knee flexion angles [25], [26]. Hence, peak muscle activations from the specified interval were analysed for its relation to trunk and knee joint angles besides interaction forces from load cells. We hypothesize that joint angles of trunk or knee are directly proportional to muscle activations whereas interaction forces and muscle activations are inversely related.

Data processing were implemented in MATLAB R2022b (MathWorks, Natick, Massachusetts, USA). Data from load cells and markers were resampled to 50Hz for uniform comparison of both data.

F. Statistical Analysis

Statistical observations were performed for peak load cell forces, marker forces and muscle activations. All data were analysed in SPSS statistics 29.0.1.0 (IBM Corp, USA). Significance level (α) of < 0.05 was used. If the data were normally distributed, ANOVA analysis followed by a post hoc Tukey test was performed such as with peak normalized load cell forces of *static stoop* trials. Otherwise, a non-parametric Kruskal-Wallis test followed by a posthoc test was implemented such as with peak normalized load cell forces of *static squat* trials. No corrections were performed to handle multiple comparison problem. Paired sample t-test was performed to compare peak forces from markers with peak load cells forces of the exosuits. To find the effect of joint angles and load cell forces on peak EMG, a multiple linear regression analysis was performed. Peak EMG was the dependent variable and trunk and knee flexion angles were the independent variables. Similarly, for finding the influence of anthropometry on measured forces, multiple linear regression analysis was performed where anthropometric measurements were the independent variables and peak normalized resultant load cell force was the dependent variable.

III. Results

The measured EMG data from left LL muscle for one subject for all the trials and load cell data for all squat trials for another subject were excluded due to noise and indistinguishable task repetitions.

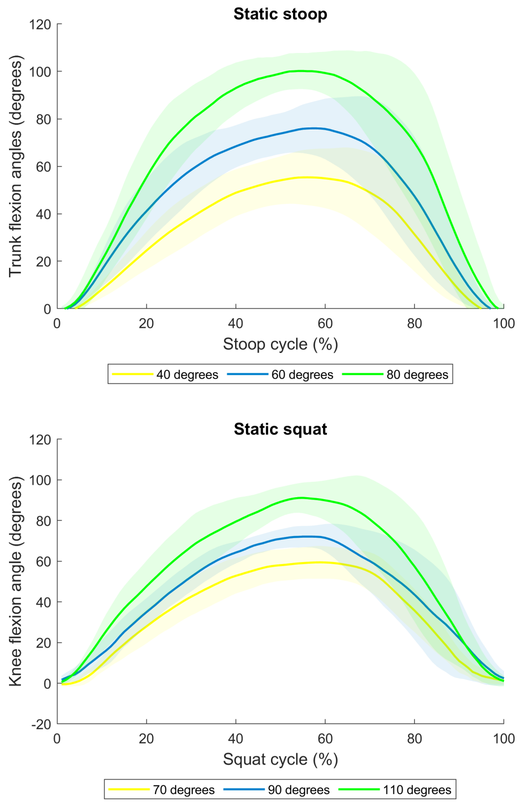

Fig. 3: Mean and std of a) trunk flexion angles of *static stoop* trials. b) knee flexion angles of *static squat* trials.

The terms interaction forces, assistive forces, exosuit forces and device-to-body forces are used interchangebly and mean the same as forces exerted by the exosuit on the user.

Figure 3 shows mean trunk and knee flexion angles across participants measured through marker trajectories during *static hold* trials. The mean trunk and knee flexion angles are deviated by a margin of 10 to 15° from the angles instructed to the users to remain at using real-time IMU data. Despite the variations, the angles are approximately 20° apart which corresponds to the objective behind these trials. For simplicity, the trials will remain as *stoop40*, *stoop60*, *stoop80*, *squat70*, *squat90* and *squat110* henceforth, as described in the experiment protocol.

A. Interaction forces from load cells

In this section, the interaction forces were compared across *static stoop* and *static squat* trials separately for both exosuits. The peak normalized resultant force obtained across all participants are represented in box plots as shown in Figure 4. In Darwing, forces from *static stoop* trials increase sequentially with respect to increase in trunk inclination in both exosuits. However, forces obtained by the users at *stoop40* and *stoop80* were only statistically significant. Similarly, *static squat* trials show gradual increase with rise in knee flexion angles. In Auxivo, forces increment with rise in trunk flexion angles but such a pattern is not observed with increase in knee flexion angles. Furthermore, the forces across the *static squat* trials were not statistically different in both exosuit conditions. It can also be observed that the peak forces obtained during *static stoop* trials are higher than those obtained during *static squat* trials in both exosuits. Statistical analysis comparing forces at *stoop80* and *squat110* in both exosuits separately, showed significant differences between the two conditions.

B. Interaction forces from marker-based method

Forces from load cells and marker-based method were analysed for *dynamic stoop* and *squat* trials. Figure 5 shows the mean interaction forces across all participants measured through load cells and marker-based method. The forces from the elastic bands on both sides of the exosuits were summed. The figure shows that the forces reach their peak between 10-30% during the first lifting cycle and between 70-90% during the second lifting cycle. In Darwing, the forces from the two methods for both trials almost overlap with each other with load cell forces being slightly higher. No significant differences in forces were found between the methods. In Auxivo, load cell forces were greater in magnitude when compared to marker-based forces. Significant differences in forces were found for both trials between the two methods.

Figure 6 shows the force-angle relationship to compare the apparent assistance provided by the exosuit through load cell and marker-based method. The assistive forces plotted were extracted from the first lifting cycle of the *dynamic* tasks where the user flexed down to pick up the box and extended back to neutral standing position. Since, significant differences were found for trials using Auxivo, only these were considered for analysis in this section. From the figure it can be observed that in both trials, load cells forces are higher than marker forces. However,the work done by these forces on the user could provide more useful insights on their performance. The work done is measured through calculating the area under the hysteresis curve. Table 2 shows the work done by these forces during different *dynamic* tasks.
For *dynamic stoop*, the work done by markers forces are marginally higher than load cell forces with a difference of 1.59%. For *dynamic squat*, the work done by load cell forces are more than markers with a difference of 21.74%. Although, both load cells and markers forces are notably different in magnitude, the work done by the forces on the user are similar to one another.

C. Influence of interaction forces and joint angles on EMG

In this section, the interaction forces from all *static hold trials* along with trunk and knee flexion angles were assessed for its influence on muscle activations. Interaction forces and trunk flexion angles were assessed for *static stoop* trials whereas interaction forces and knee flexion angles were analysed for *static squat* trials. The mean and standard deviation of muscle activations for both exosuits

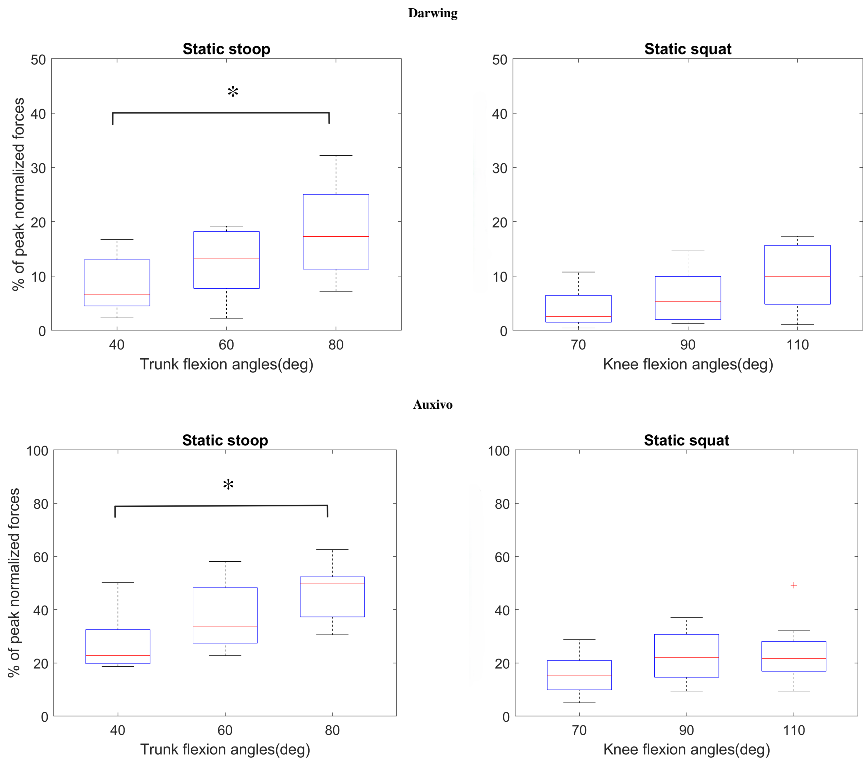

Fig. 4: Box plots representing peak normalized exosuit forces during static hold trials. The * indicates significant differences between the trials it is mentioned across.

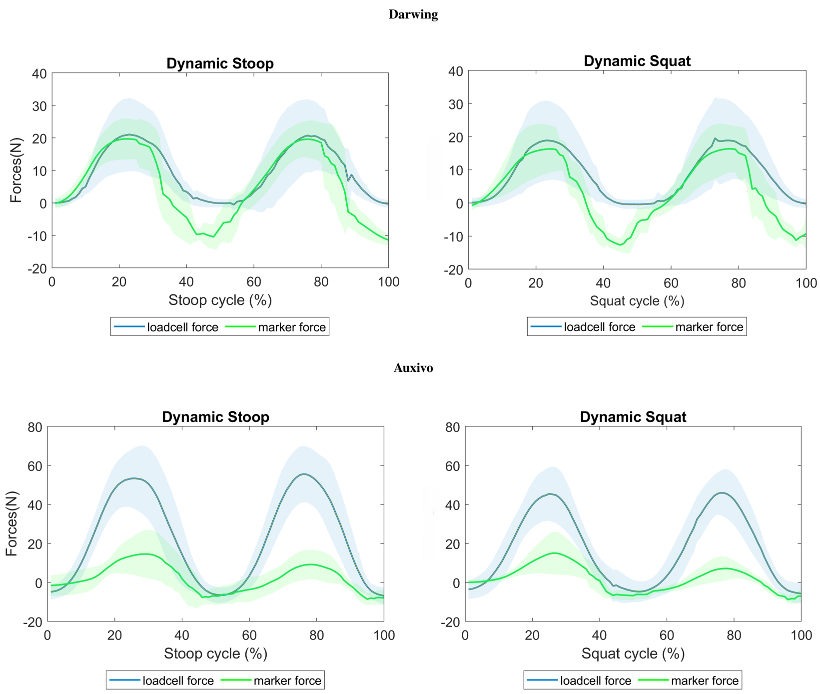

Fig. 5: Plots representing mean exosuit forces measured through load cell and marker positions for dynamic trials

TABLE II: Work done by load cells and markers forces during dynamic trials

	Work done by load cells (Nrad)	**Work done by markers (Nrad)**	**% difference in work done between both sensors**
Dynamic Stoop	284.66	289.27	1.59%
Dynamic Squat	112.06	87.70	21.74%

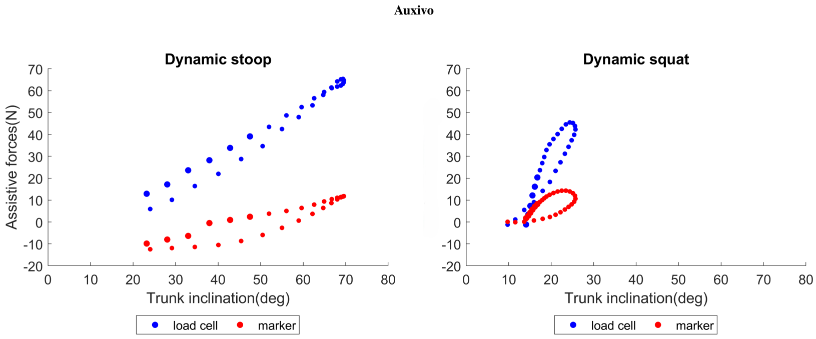

Fig. 6: Scatterplots showing assistive forces measured by load cell and marker method for dynamic trials with Auxivo. The loading phase is denoted by thicker dots and unloading phase by thinner dots of the first lifting cycle.

during *static hold trials* across all participants are shown in Appendix A. Peak muscle activation between 40-70% of the task cycle and the corresponding peak trunk or knee joint angle and load cell force were extracted and were fed as an input to the multiple linear regression model. Based on the assumptions mentioned previously, we expect to see positive linear correlation between joint angles and EMG and negative linear correlation between interaction forces and EMG. Table 3 shows the results of the regression model. The Pearson's correlation values obtained between the independent and the dependent variable are presented. Significance in correlations are mentioned in square brackets. All *static squat* trials with both exosuits did not present any significant correlation with the independent variables. Trials with Darwing showed positive correlation between IL-R muscle activation and interaction force at *stoop40* whereas negative correlation at *stoop80*. No significant interaction force influence on the muscles at *stoop60*. With respect to trunk flexion angles, LT-L,IL-R showed positive correlation at *stoop40* and LT-R,LT-L showed positive correlation at *stoop60*. The trunk flexion angles showed no significant effect on muscles at *stoop80*. Trials with Auxivo presented significant negative correlation with interaction forces at *stoop60* with LT-R.
With respect to trunk flexion angles, LT-L,IL-R showed positive correlations at *stoop40* and LT-R showed negative correlation at *stoop80*. Overall, the effect of both joint angles and interaction forces on muscle activations were minimal with neither of them having an effect on the LL muscles across all trials with both exosuits. Moreover, out of the three significant correlations of interaction forces with muscle activations, two were negative which corresponded to the initial hypotheses. All significant correlations of trunk flexion angles with muscle activations were positive as hypothesized except for one in *stoop80* with Auxivo.

D. Interaction forces and EMG for dynamic tasks

Figure 7 shows RMS EMG of the whole lifting cycle across participants for *dynamic stoop* and *squat* trials of both exosuits. Visually, the difference in RMS EMG values for both trials are small. In Darwing, RMS EMG of *dynamic squat* are higher in LL muscles and across the remaining muscles, RMS EMG of *dynamic stoop* are higher. However, no significant differences were obtained. In Auxivo, LT muscles show higher RMS EMG values for *dynamic stoop* and the rest show high values for *dynamic squat*. Significant difference in RMS EMG values were observed only for LT-L muscle. In sum, both *dynamic stoop* and *squat* lifting movements faintly increase the muscle activation of the specific back muscles.

E. Interaction forces and anthropometry

The anthropometric measurements included height, weight, trunk length, shoulder width, pelvis width and trunk to height ratio measured across all participants. Figure B.1(Appendix B) shows that the measured interaction forces from both exosuits varied across different subjects. Hence, the anthropometry was related to the interaction forces obtained from *stoop40* with both exosuits using multiple linear regression model. Table 4 shows the pearson's correlation with its significance between the various independent variables and the dependent variable. In both exosuits, only shoulder width shows significance positive correlation which means only shoulder width influences the exosuit assistance provided to the user.

IV. Discussion

In this article, a system with conventional force sensors was designed to directly measure the human-exosuit interaction forces from industrial exosuits. The sensor-based system was compared to the marker-based force estimations. Furthermore, the effect of these interaction forces on physiological parameters such as back muscle activations and anthropometry was analysed.

Figure 3 shows variation from the expected trunk and knee flexion angles measured using marker trajectories. In Figure 3a, the variation in measured trunk flexion angles could be caused by IMU sensor placement on the lumbar region. Repeated or maximum forward bending could cause the IMU to be misplaced or slip from its position, leading to drift in measured values. Another possibility could be the placement of pelvis markers on the exosuit

TABLE III: Comparing the effects of load cell forces and trunk and knee flexion angles on muscle activations through multiple linear regression model.

DARWING	Stoop40					Stoop60					Stoop80				
	LT-R	LT-L	LL-R	LL-L	IL-R	LT-R	LT-L	LL-R	LL-L	IL-R	LT-R	LT-L	LL-R	LL-L	IL-R
Interaction forces	0.37	0.37	0.30	-0.39	**0.59**	0.47	0.44	0.21	-0.35	0.29	-0.11	0.02	-0.23	-0.32	**-0.67**
	[0.10]	[0.16]	[0.46]	[0.16]	**[0.04]**	[0.09]	[0.11]	[0.28]	[0.21]	[0.21]	[0.38]	[0.47]	[0.27]	[0.23]	**[0.02]**
Trunk flexion angles	0.52	**0.62**	0.62	-0.25	**0.69**	**0.66**	**0.69**	0.30	-0.53	0.36	-0.31	0.23	-0.10	-0.26	-0.08
	[0.77]	**[0.03]**	[0.65]	[0.27]	**[0.01]**	**[0.02]**	**[0.01]**	[0.21]	[0.10]	[0.16]	[0.20]	[0.26]	[0.39]	[0.28]	[0.41]

DARWING	Squat70					Squat90					Squat110				
	LT-R	LT-L	LL-R	LL-L	IL-R	LT-R	LT-L	LL-R	LL-L	IL-R	LT-R	LT-L	LL-R	LL-L	IL-R
Interaction forces	0.19	0.20	0.08	0.15	-0.16	-0.26	0.01	-0.26	-0.18	-0.38	0.14	0.39	0.04	0.14	0.14
	[0.32]	[0.08]	[0.42]	[0.37]	[0.34]	[0.26]	[0.49]	[0.26]	[0.34]	[0.17]	[0.37]	[0.16]	[0.46]	[0.38]	[0.36]
Knee flexion angles	0.14	0.55	0.09	0.29	0.04	-0.02	0.53	0.52	0.57	0.51	-0.55	-0.24	-0.28	-0.03	-0.33
	[0.36]	[0.07]	[0.41]	[0.25]	[0.45]	[0.47]	[0.08]	[0.09]	[0.08]	[0.09]	[0.07]	[0.27]	[0.24]	[0.47]	[0.20]

AUXIVO	Stoop40					Stoop60					Stoop80				
	LT-R	LT-L	LL-R	LL-L	IL-R	LT-R	LT-L	LL-R	LL-L	IL-R	LT-R	LT-L	LL-R	LL-L	IL-R
Interaction forces	-0.09	0.28	0.21	0.45	0.50	**-0.63**	-0.25	-0.18	-0.18	-0.26	-0.42	0.44	-0.44	0.03	-0.11
	[0.41]	[0.24]	[0.30]	[0.15]	[0.10]	**[0.04]**	[0.27]	[0.33]	[0.34]	[0.28]	[0.13]	[0.11]	[0.11]	[0.46]	[0.38]
Trunk flexion angles	0.24	**0.64**	0.33	0.63	**0.69**	-0.53	-0.06	-0.31	-0.26	-0.51	**-0.71**	-0.06	-0.07	0.10	-0.25
	[0.28]	**[0.04]**	[0.21]	[0.06]	**[0.02]**	[0.08]	[0.44]	[0.22]	[0.28]	[0.11]	**[0.01]**	[0.43]	[0.42]	[0.40]	[0.25]

AUXIVO	Squat70					Squat90					Squat110				
	LT-R	LT-L	LL-R	LL-L	IL-R	LT-R	LT-L	LL-R	LL-L	IL-R	LT-R	LT-L	LL-R	LL-L	IL-R
Interaction forces	0.15	0.12	0.02	0.16	-0.14	-0.06	0.15	-0.08	0.15	-0.22	-0.40	-0.18	-0.37	-0.22	-0.37
	[0.36]	[0.38]	[0.47]	[0.35]	[0.37]	[0.44]	[0.35]	[0.41]	[0.37]	[0.29]	[0.15]	[0.33]	[0.17]	[0.31]	[0.17]
Knee flexion angles	0.17	0.57	0.15	0.45	0.36	0.20	0.51	0.18	0.50	0.30	-0.44	0.08	-0.43	0.29	-0.48
	[0.34]	[0.06]	[0.35]	[0.15]	[0.18]	[0.31]	[0.09]	[0.33]	[0.12]	[0.22]	[0.13]	[0.33]	[0.14]	[0.26]	[0.11]

The table shows Pearson's correlation between the independent and the dependent variable and the corresponding p-value is mentioned in square brackets. Significant correlations < 0.05 are highlighted in bold. LT-R,LT-L,LL-R,LL-L,IL-R are the back muscles involved.

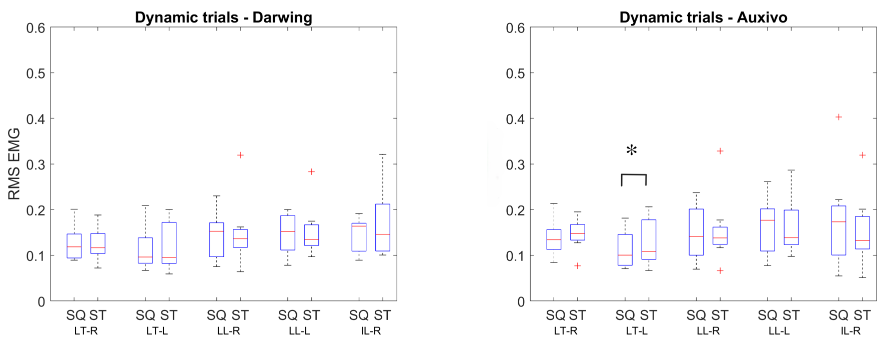

Fig. 7: Plots showing RMS EMG of the whole lifting cycle for dynamic trials of both exosuits. SQ represents dynamic squat and ST represents dynamic stoop. LT-R, LT-L, LL-R, LL-L, IL-R are the back muscles involved. * represents the significance across the trials it is mentioned.

TABLE IV: Pearson's correlation with its significance in square bracket for establishing relation between anthropometry and interaction forces for *stoop40*

Measurements	**Stoop40 (Darwing)**	**Stoop40 (Auxivo)**
Height (cm)	0.080 [0.419]	0.031 [0.469]
Weight (kg)	-0.164 [0.337]	-0.187 [0.315]
Pelvis width (cm)	-0.261 [0.249]	-0.040 [0.459]
Trunk length (cm)	-0.243 [0.265]	-0.265 [0.246]
Shoulder width (cm)	**0.654 [0.028]**	**0.828 [0.003]**
Trunk to height ratio	-0.297 [0.219]	-0.433 [0.122]

instead of bony landmarks that could cause variations in computed angles. Similarly for knee flexion angles (Figure 3b), the computation of angles between the IMUs placed on the thigh and shank could have resulted in an offset, that caused variations in the angle observed. Moreover, the participants did not flex to the predefined angles by looking at the data themselves but were rather instructed by the experimenter which could have caused delay in the system.

The measured interaction forces (Figure 4) at different trunk flexion angles for both exosuits showed that the forces increased proportionally with increase in trunk flexion angles. As the user bent forward with every 20° increase in trunk flexion angle, the elastic band stretched even more, resulting in increased forces. However, significant increase in forces could be found only between *stoop40* and *stoop80* due to 40° difference in trunk flexion angles as opposed to 20° difference. For different knee flexion angles, Darwing showed proportional increase in forces whereas Auxivo did not. Moreover, the forces recorded at maximum knee flexion were significantly lower than the forces during maximum trunk flexion. This could be because the elastic bands considered were situated on the upper interface of both exosuits that primarily supported forward bending more than kneeling. For Darwing, however, the elastic bands are also situated on the lower half of the exosuit but forces were not recorded from those.

The maximum force generated on the user's trunk by Darwing and Auxivo were 80 N and 140 N respectively during *stoop80* (Figure 4). These are less than the forces mentioned in literature. A study utilizing low-profile elastic exosuit with a moment arm of 0.08 m reported exosuit forces between 150 and 200 N to generate a torque in the range of 12-16 Nm [20]. Another study with an exosuit emulator had reported peak exosuit forces on the shoulders as 100N and on the waist as 125 N [4]. Hence, the resultant forces on the trunk sum up to 225 N. Thus, the overall exosuit forces on the trunk range above 100 N to obtain the desired torque and to reduce intense back muscle activity. Such variation in exosuit forces could be due to differences in elastic element orientation, stiffness and slack length and also the type of task the users performed. For instance, Auxivo has higher elastic band stiffness and smaller slack length [5], owing to greater forces when compared to Darwing.
Figure 5 shows the interaction forces measured from marker positions and load cells for *dynamic trials*. For Darwing, the peak interaction forces from marker positions and load cells almost overlapped with another with statistical results showing no significant difference in peak forces between the two methods. Hence, both methods can be used interchangeably to compute Darwing exosuit forces. This observation contradicts the initial hypothesis which stated that the two methods result in different forces. However, with respect to Auxivo, the peak forces from markers were significantly different from that of load cells. Marker forces were derived from elongation of the elastic bands. Hence, this variation in forces between markers and load cells is due to difference in elongation lengths between the left and right side elastic bands of Auxivo. Studies have reported previously that the thigh cuffs of Auxivo do not attach firmly on the users [5]. Since, the elastic bands are attached to these, relative movement of the cuffs on user's thigh during movement can result in uneven elongation thereby, leading to different forces on both sides. However, load cell forces were unaffected by the difference in elongation between the two elastic band and produced equal forces on both sides. As the load cell forces did not directly correspond to the stretch of the elastic bands, it is important to re-evaluate the series connection of load cells to the elastic bands in Auxivo.

The significant difference in forces between load cells and markers in Auxivo was further investigated by computing the work done by the forces from these sensors. Table 2 and Figure 6 shows that the variation in work done between the two were minimal. This is because the work done or elastic potential energy depends on stiffness and in this case, trunk inclination. Since, the two methods measured forces from same elastic band for the same movement,the work done is not different despite different magnitude of forces.

Table 3 shows the effects of interaction forces and trunk and knee flexion angles with EMG. Trunk flexion angles and interaction forces of *static stoop* trials showed significant correlations with back muscle activations for both exosuits. We hypothesized that joint angles of trunk or knee are directly proportional to muscle activations (positive correlations) whereas interaction forces and muscle activations are inversely related (negative correlations). Figure A.1, A.2 (Appendix A) shows the mean and peak EMG across all participants for *static hold trials*. From Figure A.1, we can observe that for *static stoop trials* in both exosuits, the muscle activations of certain muscles drop between 40-70% of the task cycle. This is also characterized by decline in peak EMG values of such muscles in Figure A.2 with increase in trunk flexion angles. This occurs as a consequence of flexion-relaxation phenomenon (FRP). FRP results in sudden silencing of electrical activity of erector spinae (ES) muscles during deep trunk flexion postures usually above 75° [27], [28] due to load sharing between the muscles and surrounding passive tissues [29], [30]. While comparing Figure A.1 and Table 3, we can observe that the muscles that were not affected by FRP mostly showed positive significant correlations with trunk flexion angles. For instance, in Darwing, LT-L, IL-R in *stoop40* and LT-R, LT-L in *stoop60*. This is because these muscles show high peak EMG value during the highest trunk flexion angle of each trial, thereby positive linear relationship with trunk flexion angles are established. On the contrary, FRP reduces the peak EMG between 40-70% of the task cycle and more negative correlations although not significant (except LT-R in Auxivo *stoop80*), can be observed with increase in trunk flexion angles for both exosuits in Table 3.

Some studies showed that FRP occurs when the trunk is flexed in the range of 75 to 90° [31], [32]. However, another study evaluating the upper body flexibility of young males reported that low flexibility is associated with early onset of FRP at trunk flexion angles as low as 30° [33]. In Figure A.1, LL muscles slightly begin to undergo FRP right from *stoop40* in both exosuits. Hence, it is possible that the participants recruited in the study are likely to fall under moderate to low trunk flexibility category due to early FRP detection. This conclusion can be supplemented by the inability of some subjects to perform *stoop60* and *stoop80* without bending their knees [34].

Another plausible explanation for the existence FRP at low flexion angles can be based on muscle recruitment pattern. A study showed that lumbar erector spinae (LES) are recruited first followed by thoracic erector spinae (TES) during forward bending [30]. Hence, LL muscle activations saturate and start to drop due to FRP first at low flexion angles whereas this pattern is observed in LT muscles at higher flexion angles. As an example, LT muscles in Darwing show significant positive correlations (Table 3) and high peak EMG values (Figure A.2) during *stoop40* and *stoop60* as opposed to no significant correlations observed with LL muscles throughout the range of trunk flexion angles. It is however, interesting to note that in Auxivo, LT muscles present decline in peak EMG between 40-70% of the task cycle in *stoop60*. For the same trunk flexion angle with only difference being the exosuit condition, it is probable that LT muscles or even all muscles in *stoop60* showed lower activations as they were equally influenced by interaction forces from Auxivo. This is strengthened by the presence of a significant negative correlation of LT-R muscle with interaction forces in Auxivo *stoop60* (Table 3). Nevertheless, LL muscles with Auxivo showed FRP with no significant correlations for all trunk flexion angles as Darwing.

Only two negative correlations of interaction forces and muscle activations were observed. In Darwing, a significant negative correlation was represented by IL-R in *stoop80*. Reduction in peak EMG of the specified muscle can be attributed to joint contribution from interaction forces and trunk angles. In Auxivo, as mentioned earlier, the negative correlation could have caused reduction in LT-R activity in *stoop60*. There are two possible reasons for minimal impact of interaction forces on muscle activity. First, insufficient force production in significantly reducing muscle activity by the exosuits. From Figure 4, we can observe that in Darwing, less than 50% (maximum 80 N) of the maximum force (236 N) from the exosuit were generated to the user. Auxivo generated less than 80% (maximum 140 N) of the maximum force (236 N) from the exosuit to the user. However, this contradicts previous researches that proved significant EMG reductions with these exosuits when compared to without exosuit condition [1], [5]. Hence, including other parameters such lumbar joint torque and compression loads in the regression model would be crucial to conclude the effects of interaction forces on the user. Second, loss of forces during transfer to the user [35], [36]. Figure 6 shows hysteresis of the elastic band in Auxivo that translates to loss of elastic energy or force transfer when the user extends upwards post flexion.

With respect to *static squat trials*, both exosuits did not show any significant correlations of muscle activations with knee flexion angles and interaction forces. It is also evident from Figure A.1, A.2 where the muscle activations increased with increase in knee flexion angles in both exosuits and with no visible presence of FRP. This is in accordance with results from [32] that also showed no significance of back muscles with knee flexion angles while performing different range of trunk and knee flexion angle movements.

Figure 7 shows RMS EMG across *dynamic stoop* and *squat* trials for both exosuits. Trunk flexion angles were higher in *dynamic stoop* than *dynamic squat* (Figure 4). Muscle activation increases with increase in trunk flexion angles. Hence, in Darwing and Auxivo, LT muscles show increase in RMS EMG for *dynamic stoop* than *dynamic squat*. However, LL muscles show a decrease in RMS EMG in *dynamic stoop* because of early muscle recruitment and onset of FRP at low trunk flexion angles. The differences in RMS EMG between the trials were not significant in Darwing whereas Auxivo showed significant difference for LT-L muscle. IL-R muscle in Darwing showed higher RMS EMG for *dynamic stoop* and the contrary was observed in Auxivo. It is possible that with Auxivo, IL-R was either influenced by interaction forces from the exosuit or by FRP like its lumborum equivalents.

Figure B.1 (Appendix B) shows inter-subject variability in interaction forces during *stoop40*. Table 4 shows that this variability were possibly caused due to difference in shoulder width across participants. Table B.1 (Appendix B) shows raw measurement data across the participants. While correlating Table B.1 and Figure B.1, we can observe that subjects with shoulder width above 35 cm tend to mostly receive higher forces from both exosuits whereas subjects in the lower shoulder width range (30-33cm) obtain less forces. Hence, it is important to use exosuits of different sizes such that all participants benefit from optimal assistance from the exosuits during different tasks. Heroware Apex adopted different design combinations, offering specific fit for people of different sizes [37].

A. Limitations and future work

The sample size of this study was small especially for performing regression analysis with EMG. Moreover, the male to female participant ratio was 9:1 as not many female participants could fit into the exosuits well. Hence, changes in interaction forces with respect to female anthropometric measurements are unknown or limited. Furthermore, a study showed that FRP onset is different across male and female which could not be detailed in this study [38].

The regression model was constrained to univariate analysis involving single dependent variable. However, for promising results on the effect of interaction forces and joint angles on the user, including other EMG parameters or joint torque and compression loads could be helpful. In this analysis, linear relationship between the independent and dependent variables were assumed. Pearson's correlation shows significant or high correlations only when the variables are linearly proportional to each other. However, in some cases, non-linear relationship is also possible and this could not be assessed due to time constraints. Adding to this, interaction between the independent variables (trunk, knee flexion angles and interaction forces) were significant in a few cases. This arises multicollinearity where the individual effects of the independent variables with the dependent are tampered. Although, this does not significantly affect the pearson's correlation, the regression model's overall performance (R^2) is compromised. In such cases, the independent variables can be averaged or one of the variables can be removed. More efficient method to deal with multicollinearity is to generate a new uncorrelated variable combining the variances of the independent variables using principle component analysis (PCA).

The study used regular-sized exosuits. However, the participants included in the study had varied anthropometric measurements and this lead to non-uniform exosuit forces across participants. Hence, in such cases "one-size-fits-all" approach is not advised.

The Arduino microcontroller was manually synced to Qualysis which is not ideal as some differences in milliseconds could be observed. A connection system with wires ensuring, no delay in data transmission between Arduino and Qualysis is required for proper synchronization and this could not be performed due to lack of time.

In Darwing, the load cells placed only on the upper half of the exosuit did not give a complete picture of the assistance provided by the suit. Especially for squat tasks, lower elastic bands is expected to provide more support which was not explored in this study.

Trunk and knee flexion angles measurement through marker trajectories resulted in angles different from the ones expected. Knee angles can be determined through inverse kinematics in Opensim however, trunk inclination could not be obtained through this technique. Hence, different approach such as computer vision methods or using other devices such as goniometers that are applicable to measuring both joint flexion angles should be adopted.

Future work can focus on estimation of L5S1 joint torques and compression loads from the available data. This can also serve as additional variables in the regression analysis. Sample size can be increased with equal distribution of male and female participants. Load cell data acquisition can be optimized by incorporating wireless transmission of force data with simulated circuit representation. This eradicates the need for using two different software for data acquisition and data storing. As the components used in the circuit are fragile and can be damaged easily with prolonged use, online simulation of the circuit connections can be helpful.

V. Conclusion

In this study, the two industrial exosuit forces were measured using force sensors to measure forces exerted by the exosuits on the user. The obtained exosuit forces were compared to marker-based force estimation and assessed for EMG and user's anthropometry. The exosuits were suitable for stoop than squat tasks due to higher assistance to the user. Measurement of forces through load cells and marker-based methods for Auxivo were different and requires re-evaluation. Effects of trunk flexion angles on EMG overpowered that of interaction forces on EMG whereas knee flexion angles had no significant impact on EMG. Difference in shoulder width affected exosuit forces across participants, signifying the need for using exosuits of different sizes. The study hopefully provided detailed performance analysis of the two exosuits during different industry tasks that can pave way for future developments to enhance optimal assistance to the users.

VI. External collaborations

The study involved companies namely: Pre-Tec exoskeletons, Nijverdal, the Netherlands (distributor of Darwing exosuit) and Daiya Industry Co., Ltd, Okayama, Japan (manufacturer of Darwing exosuit).

VII. AI USE

"During the preparation of this work the author(s) used ChatGPT for LaTEX support and grammar checking. After using this tools, the author(s) reviewed and edited the content as needed and take(s) full responsibility for the content of the work."

References

[1] R. M. van Sluijs, M. Wehrli, A. Brunner, and O. Lambercy, "Evaluation of the physiological benefits of a passive back-support exoskeleton during lifting and working in forward leaning postures," *Journal of Biomechanics*, vol. 149, p. 111489, 2023.

[2] S. Madinei and M. A. Nussbaum, "Estimating lumbar spine loading when using back-support exoskeletons in lifting tasks," *Journal of Biomechanics*, vol. 147, p. 111439, 2023.

[3] W. T. R., P.-A. Vern, G. Arun, and F. L. J., "Revised niosh equation for the design and evaluation of manual lifting tasks," *Ergonomics*, vol. 36, pp. 749–776, 1993.

[4] S. Bhardwaj, A. B. Shinde, R. Singh, and V. Vashista, "Manipulating device-to-body forces in passive exosuit: An experimental investigation on the effect of moment arm orientation using passive back-assist exosuit emulator," *Wearable Technologies*, vol. 4, p. e17, 2023.

[5] M. I. M. Refai, A. Moya-Esteban, L. van Zijl, H. van der Kooij, and M. Sartori, "Benchmarking commercially available soft and rigid passive back exoskeletons for an industrial workplace," *Wearable technologies*, vol. 5, p. e6, 2024.

[6] M. Abdoli-Eramaki, J. M. Stevenson, S. A. Reid, and T. J. Bryant, "Mathematical and empirical proof of principle for an on-body personal lift augmentation device (plad)," *Journal of Biomechanics*, vol. 40, no. 8, pp. 1694–1700, 2007.

[7] E. P. Lamers, A. J. Yang, and K. E. Zelik, "Feasibility of a biomechanically-assistive garment to reduce low back loading during leaning and lifting," *IEEE Transactions on Biomedical Engineering*, vol. 65, no. 8, pp. 1674–1680, 2018.

[8] M. Goršič, Y. Song, B. Dai, and D. Novak, "Evaluation of the herowear apex back-assist exosuit during multiple brief tasks," *Journal of Biomechanics*, vol. 126, p. 110620, 2021.

[9] M. B. Yandell, D. M. Ziemnicki, K. A. McDonald, and K. E. Zelik, "Characterizing the comfort limits of forces applied to the shoulders, thigh and shank to inform exosuit design." *PloS one*, vol. 15(2), p. e0228536, 2020.

[10] E. P. Lamers and K. E. Zelik, "Design, modeling, and demonstration of a new dual-mode back-assist exosuit with extension mechanism," *Wearable Technologies*, vol. 2, p. e1, 2021.

[11] M. Pang, Z. Luo, B. Tang, J. Luo, and K. Xiang, "Estimation of the interaction force between human and passive lower limb exoskeleton device during level ground walking," *Biomimetic Intelligence and Robotics*, vol. 2, no. 3, p. 100056, 2022.

[12] P.-L. Liu, C.-C. Chang, H.-Y. Kao, and C.-Y. Hsiao, "Artificial neural network can improve the accuracy of a markerless skeletal model in l5/s1 position estimation during symmetric lifting," *Journal of Biomechanics*, vol. 130, p. 110844, 2022.

[13] S. André, "An explicit model to predict and interpret constraint force creation in phri with exoskeletons," in *IEEE International Conference on Robotics and Automation*, 2008, pp. 1324 – 1330.

[14] D. Scherb, S. Wartzack, and J. Miehling, "Modelling the interaction between wearable assistive devices and digital human models—a systematic review," *Frontiers in Bioengineering and Biotechnology*, vol. 10, 2023.

[15] M. Stefano, R.-C. David, P.-F. David, M. J. C., L. Matteo, and T. Diego, "Characterization and evaluation of human–exoskeleton interaction dynamics: A review," *Sensors*, vol. 22, no. 11, 2022.

[16] R. Ashish, W. Matthew, M. R. Dafne, L. Rui, and C. Tom, "Quantifying the human-robot interaction forces between a lower limb exoskeleton and healthy users," *IEEE Engineering in Medicine and Biology Society*, vol. 2016, pp. 586–589, 08 2016.

[17] S. D. Rossi, N. Vitiello, T. Lenzi, R. Ronsse, B. Koopman, A. Persichetti, F. Giovacchini, F. Vecchi, A. Ijspeert, H. van der Kooij, and M. Carrozza, "Soft artificial tactile sensors for the measurement of human-robot interaction in the rehabilitation of the lower limb," *IEEE Engineering in Medicine and Biology Society*, vol. 2010, pp. 1279–82, 08 2010.

[18] A. L. E., Q. Fernandez, G. X., C. A., and A. J., "Study of patient-orthosis interaction forces in rehabilitation therapies," in *Biomedical Robotics and Biomechatronics (BioRob)*, 2012, pp. 1098–1103.

[19] M. Abdoli-E, M. J. Agnew, and J. M. Stevenson, "An on-body personal lift augmentation device (plad) reduces emg amplitude of erector spinae during lifting tasks," *Clinical Biomechanics*, vol. 21, pp. 456–465, 2006.

[20] E. P. Lamers, J. C. Soltys, A. J. Yang, and K. E. Zelik, "Low-profile elastic exosuit reduces back muscle fatigue," *Sci Rep*, vol. 10, 2020.

[21] K. Vijay, shinde Vasudev, and K. Jayant, "Overview of load cells," *Mechanical and mechanics engineering*, vol. 6, 10 2021.

[22] S. Al-Mutlaq and A. the Giant, "Load cell amplifier hx711 breakout hookup guide." [Online]. Available: https://learn.sparkfun.com/tutorials/load-cell-amplifier-hx711-breakout-hookup-guide/all

[23] J. Gaudet and G. Handrigan, "Assessing the validity and reliability of a low-cost microcontroller-based load cell amplifier for measuring lower limb and upper limb muscular force." *Sensors (Basel, Switzerland)*, vol. 20(17), 2020.

[24] J. H. van Dieën, M. J. Hoozemans, and H. M. Toussaint, "Stoop or squat: a review of biomechanical studies on lifting technique," *Clinical Biomechanics*, vol. 14, no. 10, pp. 685–696, 1999.

[25] S.-K. Lee and D.-J. Park, "The effects of knee joint and hip abduction angles on the activation of cervical and abdominal muscles during bridging exercises," *Journal of Physical Therapy Science*, vol. 25, no. 7, pp. 857–860, 2013.

[26] G. Shin, Y. Shu, Z. Li, Z. Jiang, and G. Mirka, "Influence of knee angle and individual flexibility on the flexion–relaxation response of the low back musculature," *Journal of Electromyography and Kinesiology*, vol. 14, no. 4, pp. 485–494, 2004.

[27] W. Floyd and P. Silver, "Function of erectores spinÆ in flexion of the trunk," *The Lancet*, vol. 257, pp. 133–134, 1951.

[28] M. Ramezani, A. Kordi Yoosefinejad, and A. Motealleh, "Comparison of flexion relaxation phenomenon between female yogis and matched non-athlete group," *BMC Sports Sci Med Rehabil*, vol. 14, 2022.

[29] A. Gouteron, A. Tabard-Fougère, and A. Bourredjem, "The flexion relaxation phenomenon in nonspecific chronic low back pain: prevalence, reproducibility and flexion–extension ratios. a systematic review and meta-analysis," *Eur Spine J*, vol. 31, p. 136–151, 2022.

[30] Y.-L. Chen, Y.-M. Hu, Y.-C. Chuan, T.-C. Wang, and Y. Chen, "Flexibility measurement affecting the reduction pattern of back muscle activation during trunk flexion," *Appl. Sci*, vol. 10, 2020.

[31] Y.-L. Chen, L.-S. Huang, L.-W. Peng, and L.-J. Shi, "Bowing with a trunk flexion of 90°: Perspectives on consumers and service personnel," *International Journal of Industrial Ergonomics*, 02 2015.

[32] G. Shin, Y. Shu, Z. Li, Z. Jiang, and G. Mirka, "Influence of knee angle and individual flexibility on the flexion–relaxation response of the low back musculature," *Journal of Electromyography and Kinesiology*, vol. 14, no. 4, pp. 485–494, 2004.

[33] W. C. L. Y. H. Chen, Y. L.and Lin, Y. Chen, and P. Y. Kang, "Changing the pattern of the back-muscle flexion-relaxation phenomenon through flexibility training in relatively inflexible young men," *PloS one*, 2021.

[34] Y. L. Chen and Y. H. Liao, "Differential back muscle flexion-relaxation phenomenon in constrained versus unconstrained leg postures," *Bioengineering (Basel, Switzerland)*, 2024.

[35] G. Song, J. Moon, J. Kim, and G. Lee, "Development of quasi-passive back-support exoskeleton with compact variable gravity compensation module and bio-inspired hip joint mechanism," *Biomimetics*, vol. 9, 2024.

[36] A. N. Cuttilan, R. F. Natividad, and R. C.-H. Yeow, "Fabric-based, pneumatic exosuit for lower-back support in manual-handling tasks," *Actuators*, vol. 12, 2023.

[37] G. Ashta, S. Finco, D. Battini, and A. Persona, "Passive exoskeletons to enhance workforce sustainability: Literature review and future research agenda," *Sustainability*, vol. 15, 2023.

[38] M. Solomonow, R. V. Baratta, A. Banks, C. Freudenberger, and B. H. Zhou, "Flexion–relaxation response to static lumbar flexion in males and females," *Clinical Biomechanics*, vol. 18, no. 4, pp. 273–279, 2003.

APPENDIX A

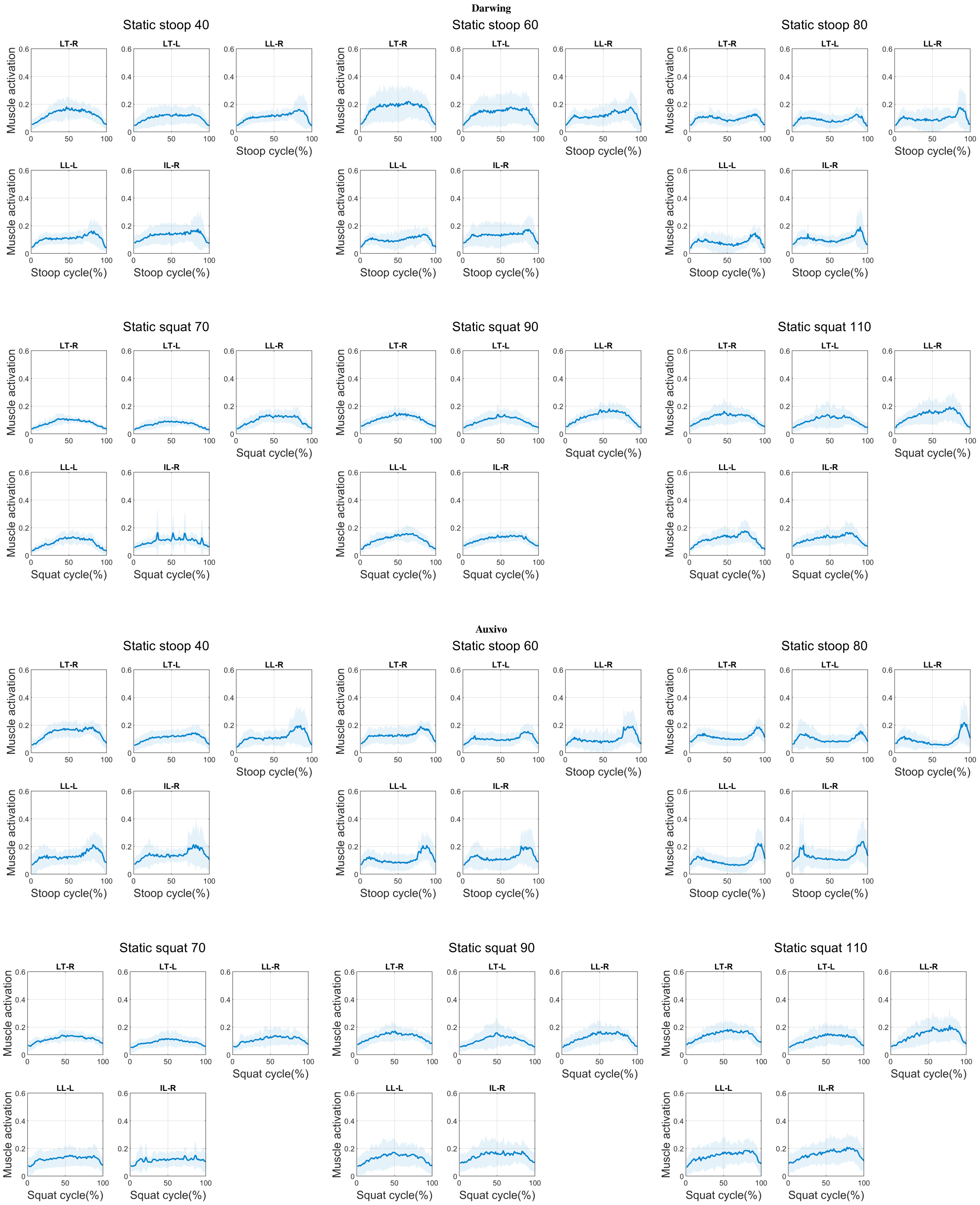

Fig. A.1: EMG envelopes for static hold trials.

Darwing

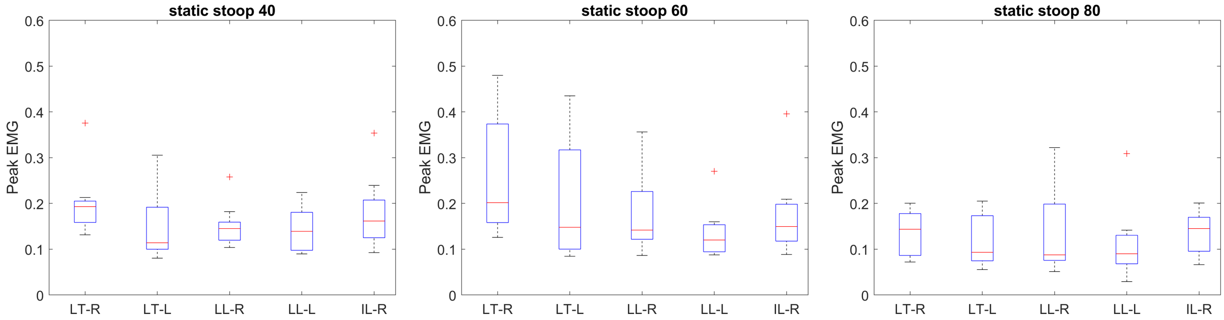

Auxivo

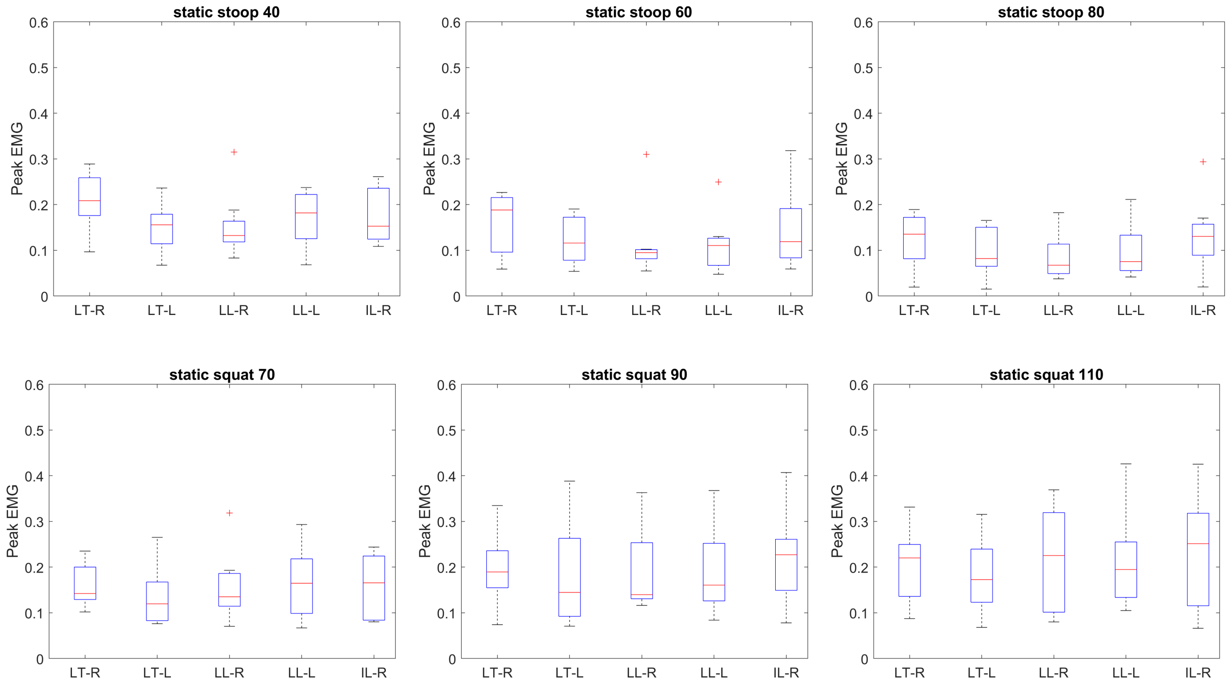

Fig. A.2: Peak EMG for static hold trials.

APPENDIX B

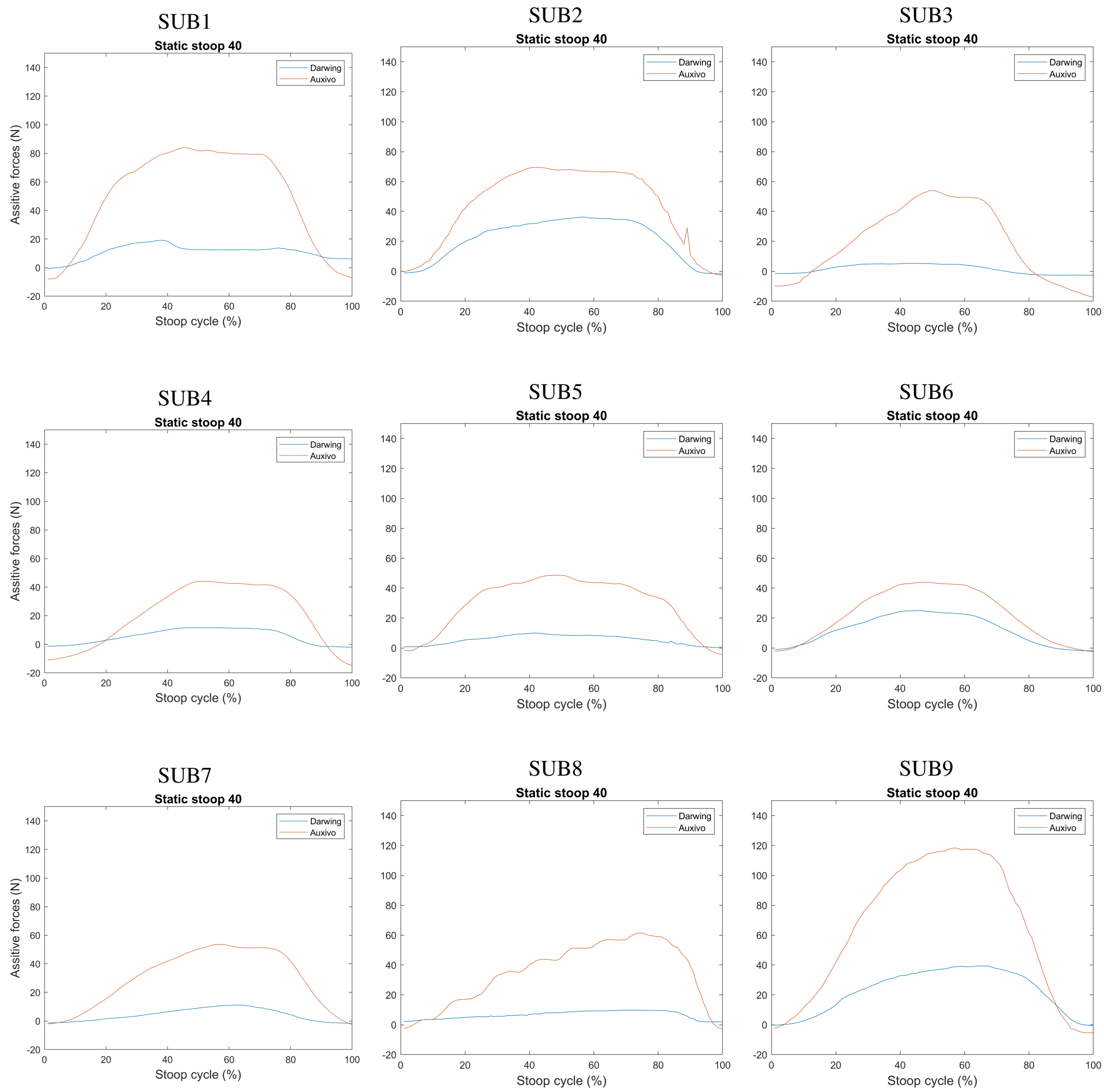

Fig. B.1: Interaction forces measured from load cells with right and left side forces summed. The forces from each subject are presented for *stoop40* trial with Darwing and Auxivo

TABLE B.I: Anthropometric measurements of participants in the study

Subject number	Height (cm)	Weight (kg)	Trunk length (cm)	Pelvis width (cm)	Shoulder width (cm)	Trunk to height ratio
1	182	75	44.01	28.35	36.53	0.24
2	182	75	44.57	22.73	37.28	0.24
3	185	70	47.95	27.94	33.69	0.26
4	193	115	51.79	36.06	34.66	0.27
5	163	57	41.28	18.63	31.75	0.25
6	166	65	44.03	24.78	30.62	0.26
7	165	70	45.13	24.86	31.38	0.27
8	165	70	42.38	28.20	32.50	0.25
9	167	64	43.60	25.23	38.37	0.26

APPENDIX C - CASE STUDY

This section deals with data collected from the aged participant outside UT. The collected data could not be combined with that of young population because the EMG parameters of the old people are differ from the ones observed in young people [1]. Figure C.1 and C.2 depict mean and peak EMG for static hold trials of the aged participant respectively. From both figures,we can observe that the FRP is not visibly present in LL muscles for low trunk flexion angles (*stoop40* and *stoop60*) whereas the young population presented FRP at low flexion angles itself (Figure A.1 and A.2). These findings are consistent with the results obtained from another study that showed that for people over 40 years of age, back extensor muscle activity remained heightened throughout the range of trunk motion to protect the surrounding passive structures whereas the opposite behaviour was presented in young adults [1].

With respect to knee flexion angles, FRP can be visually observed for *squat90* and *squat110* for both exosuits whereas young adults did not present FRP for squat trials using both exosuits. This could be possible due to increased trunk flexion or forward trunk motion during *stoop90* and *stoop110*.

The EMG signals in Figure C.1 present some distortions. This could be because of prominent skin folds on the trunk, creating an uneven surface for the placement of sensors in old aged people.

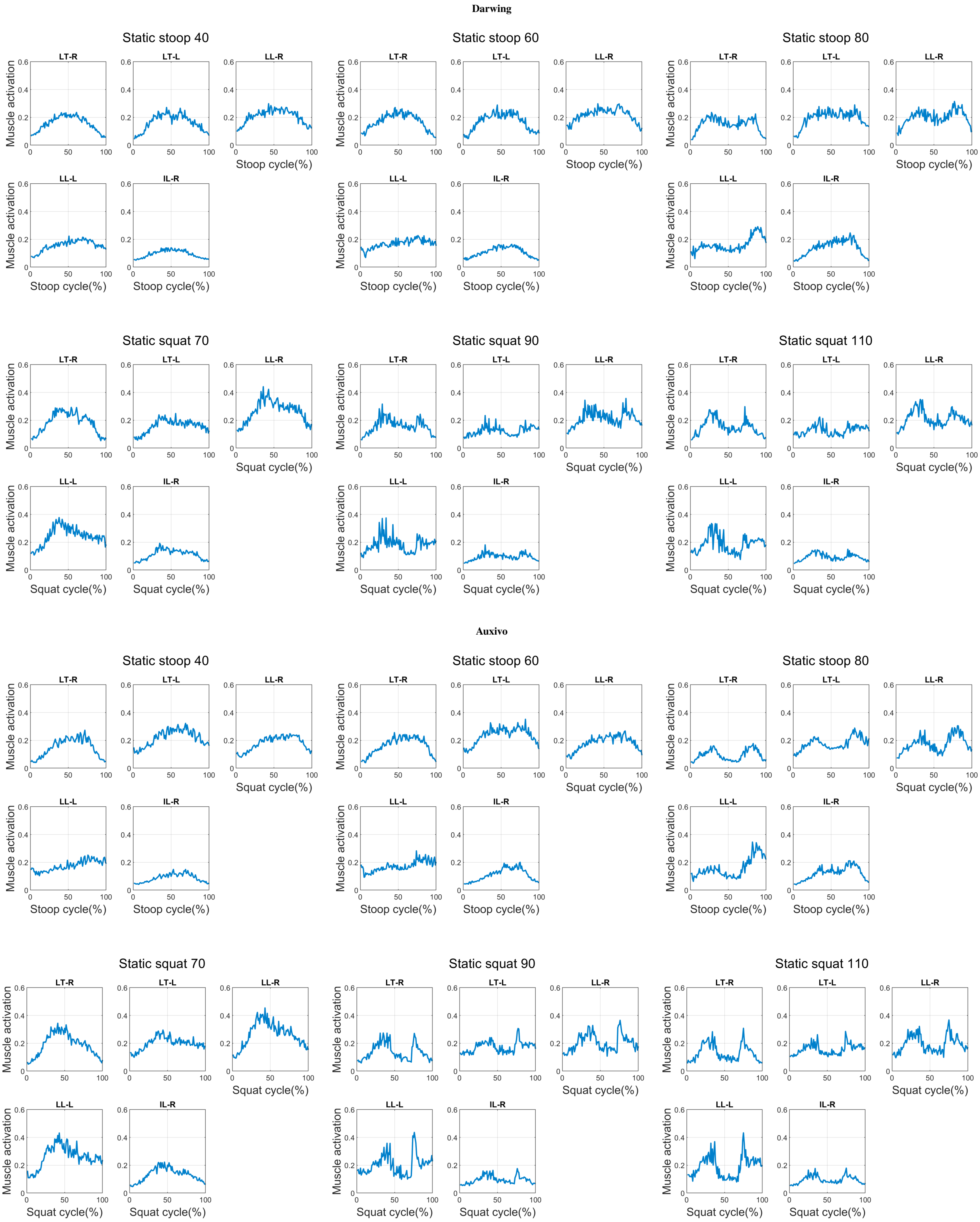

Fig. C.1: EMG envelopes for static hold trials for the aged participant.

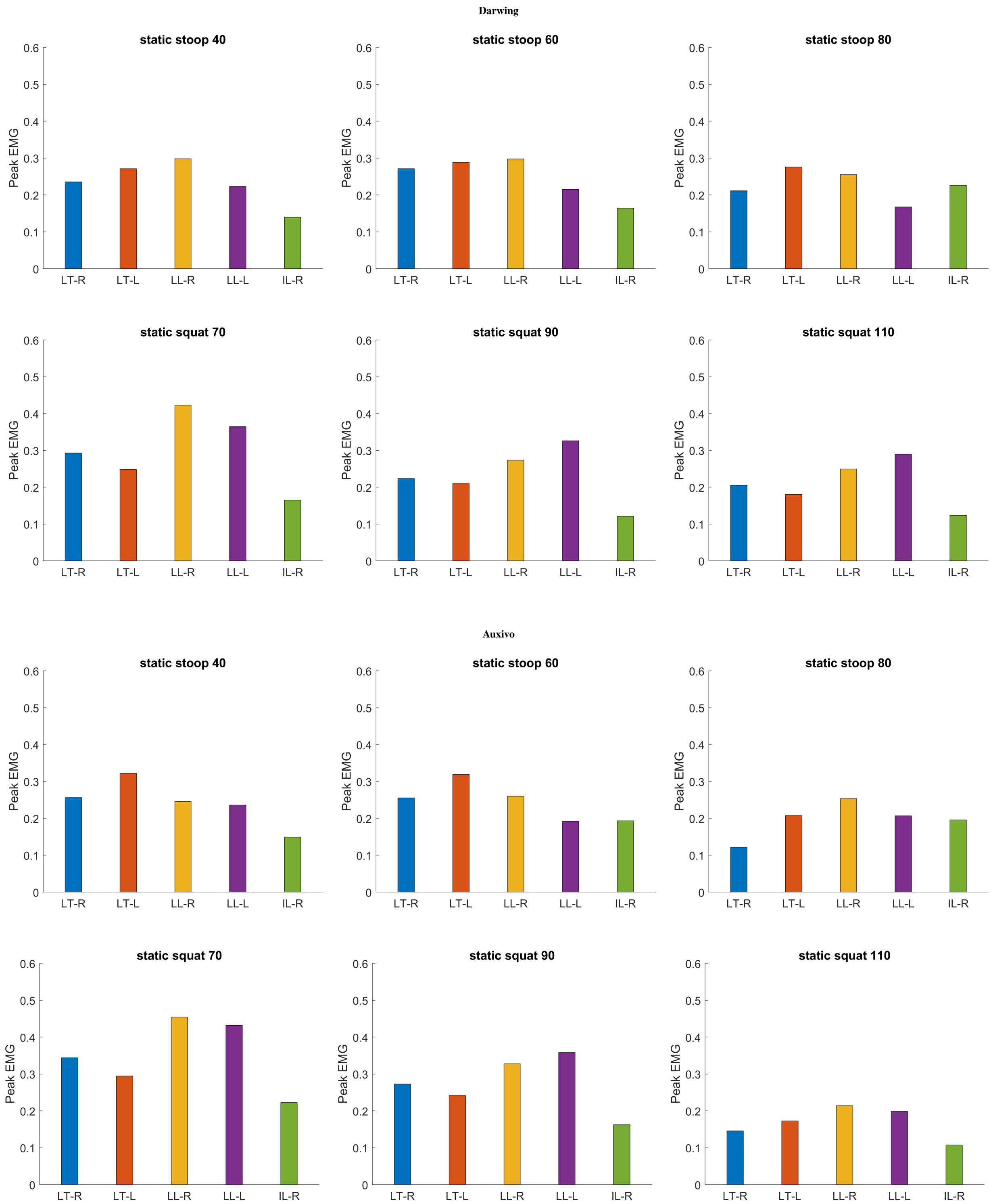

Fig. C.2: Peak EMG for static hold trials for the aged participant.

APPENDIX D - INDUSTRY IMPLEMENTATION

Force data acquisition from load cells in Darwing exosuit were implemented in an industry at Waalwijk, the Netherlands. The exosuit fitted with load cells were worn by 7 industry workers. Stoop and squat movements were performed by the users and the range of forces recorded during each movement are detailed in Table 6. The users did not stoop and squat to pre-defined angles as described in the experiment protocol. Hence, direct comparison between the forces obtained from users at the industry and laboratory could not be performed. Furthermore, the forces obtained during stoop and squat were mostly in the same range for most users. This is because some users performed a full squat (135 degree knee flexion) instead of half-squat (90-100 degree knee flexion) that gave rise to more forces and the same users performed minimal forward bending (40-60 degree trunk flexion) which resulted in moderate forces. Shoulder width of all users were greater than 35 cm and the forces were above 10N for both the tasks across all users.

Fig. D.1: Snapshots of the warehouse of the industry and workers performing tasks wearing Darwing exosuit

TABLE D.I: Subject physical characteristics and force range during stoop and squat.

Subject numbers	Height (cm)	Weight (cm)	Shoulder width (cm)	Force range during stoop (N)	Force range during squat (N)
1	187	95	37	10-15	15-25
2	187	101	45	18-25	10-15
3	178	67	45	15-20	10-15
4	177	73	38	15	14-15
5	180	85	44	20-22	22-23
6	180	73	37	20-25	19-26
7	176	80	37	20-25	15-20

References

[1] T. Zhang, A. Firouzabadi, D. Yang, S. Liu, and H. Schmidt, “Age-dependent flexion relaxation phenomenon in chronic low back pain patients,” *Frontiers in Bioengineering and Biotechnology*, 2024.